Agricultural and Forest Meteorology 358 (2024) 110247

Contents lists available at ScienceDirect

Agricultural and Forest Meteorology

journal homepage: www.elsevier.com/locate/agrformet

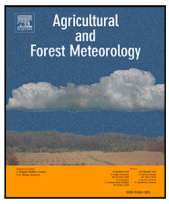

Signs of frost drought in stem diameter variations

Fabien Delapierre [a,*], Christine Moos [b], Heike Lischke [c], Patrick Fonti [d]

[a] Faculty of Geosciences and Environment, University of Lausanne, Lausanne, CH-1015, Switzerland
[b] BFH-HAFL, Bern University of Applied Sciences, Zollikofen, CH-3052, Switzerland
[c] Dynamic Macroecology, Swiss Federal Institute for Forest, Snow and Landscape Research WSL, Birmensdorf, CH-8903, Switzerland
[d] Dendrosciences, Swiss Federal Institute for Forest, Snow and Landscape Research WSL, Birmensdorf, CH-8903, Switzerland

ARTICLE INFO

Keywords:
Frost drought
Winter desiccation
Treeline
Winter
Dendrometer
Freeze–thaw cycles
Stem diameter variations

ABSTRACT

Frost drought refers to the chronic or acute desiccation of trees exposed to high evaporative pressures while being rooted in cold or frozen soils. This phenomenon has been known for more than a century but is still poorly characterized. Summer desiccation manifests itself as long-term stem contractions. Similar contractions have been reported in winter. In this study, we investigated the causes of total winter stem contraction (WSC) using 14 years of dendrometer data from evergreen (*P.abies*) and deciduous (*L.decidua*) mature trees growing along an elevational transect (from 800 to 2200 m asl) in the Swiss Alps. Results indicated that WSC varied between 30 μm and 1478 μm and were strongly dependent on species, elevation, and tree height. Moreover, the magnitude of contractions was strongly associated with stem contractions subsequent to freeze–thaw events (ΔF). We suggest that both ΔF and WSC are the consequences of water losses due to ice blockage associated frost drought, occurring when the distal parts of the tree are thawed and transpiring, while the larger basal parts remain frozen, thus inhibiting water uptake and creating a hydraulic imbalance.

1. Introduction

During winter, trees face potential threats to their structural integrity, including frost and snow damage (Sakai and Larcher, 1987; Wieser and Tausz, 2007). Additionally, despite having reduced transpiration, they can still be vulnerable to a form of drought provoked by the inhibition of soil water uptake due to low soil temperatures. This phenomenon has been known for over a century and has been reported as "Frosttrocknis", "frost drought" or "winter desiccation" (Neger, 1915; Herrick and Friedland, 1991; Mayr et al., 2006a; Tranquillini, 1982).

Despite the long and rich history of research that it has inspired, frost drought remains an elusive and poorly characterized phenomenon. A major hindrance is that visible manifestations of frost drought are difficult to observe and occur later, during the growing season (Tranquillini, 1982; Körner, 2012). Frost drought is therefore often characterized by measuring the embolization rate of xylem conduits on the branches (Tranquillini, 1982; Mayr and Charra-Vaskou, 2007; Maruta et al., 2020; Charra-Vaskou et al., 2012). However, this approach is limited by the fact that embolisms are also caused by freeze–thaw cycles, typically concomitant with frost drought (Sperry and Sullivan, 1992). Moreover, embolization might not always represent a severe threat to the water balance of trees, especially when water losses are drastically reduced as it is the case in winter (Körner, 2019).

Another difficulty is tied to the mechanistic nature of frost drought. Generally speaking, the driving forces of the water imbalance are, on the one side, water losses, driven by evaporative pressures and the tree's transpiration resistance, and, on the other side, water uptake impairment, linked to soil temperatures. These effects can vary in intensity, impacting trees in different ways and with varying severity. Accordingly, frost drought has been described both as slow and long-term "chronic" and very fast and "acute" desiccation (Sakai and Larcher, 1987).

It is commonly accepted that frost drought is particularly associated with high elevations and late winter/early spring, when both the evaporative forces (winds and solar radiation) are high and when trees are still susceptible to being rooted in frozen soils (Larcher and Siegwolf, 1985; Baig and Tranquillini, 1980; Beikircher and Mayr, 2013). However, many cases have been reported where the phenomenon deviates from this general pattern (Sakai and Larcher, 1987). For example, frost drought can even occur in warmer soil if the basal part of the stem remains frozen over long periods of time causing an "ice blockage" inhibiting water uptake (Mayr et al., 2012).

For these reasons, the ecological significance of frost drought is still heavily debated. It has been thought to be a very widespread phenomenon and perhaps the main agent behind the establishment of tree lines (Tranquillini, 1979). Others have postulated that it only

* Corresponding author.
E-mail address: f.delapierre@outlook.com (F. Delapierre).

https://doi.org/10.1016/j.agrformet.2024.110247
Received 2 April 2024; Received in revised form 9 September 2024; Accepted 25 September 2024
Available online 16 October 2024

concerned small trees above the treeline, as mature trees should have enough water reserves to compensate for the loss (Körner, 2012).

Stem diameter variations (SDV) can provide promising information to study the water status of a tree (Zweifel and Häsler, 2000). They are mainly shaped by cellular growth/death and the water content of the living bark, which is thought to shrink when the evaporative losses exceed the water uptake and to swell in the opposite scenario (Zweifel et al., 2001). In winter, SDV are also affected by freeze–thaw cycles as living cells dehydrate and contract in response to apoplastic water freezing, to protect themselves from intracellular freezing (Zweifel and Häsler, 2000; Lindfors et al., 2019; Bozonnet et al., 2024). This process is reversible: cells rehydrate and swell upon thawing. However, irreversible diameter changes may occur following cellular death. Améglio et al. (2001). So far, SDV have been mainly used to characterize the water balance of a tree in summer (Zweifel et al., 2005; Brinkmann et al., 2016; Schäfer et al., 2019). By detrending them for growth, summer droughts appear as long-term trend of contraction of the stem (Zweifel et al., 2005). A similar contraction has been observed and reported in winter and might be linked to frost drought (Loris et al., 1999).

In this article, we make use of winter stem contractions to delve into the multifaceted phenomenon of frost drought, exploring its underlying mechanisms, ecological implications, and the evolving perspectives that are reshaping our comprehension of its effects on tree physiology and distribution. Specifically, we postulated that winter stem contraction (WSC) at high elevations are indication of frost drought either induced by frozen soil or frozen xylem tissue. To discriminate between the two frost drought processes we characterized and quantified WSC using long-term monitoring of stem size variations of *P. abies* and *L. decidua* trees at different elevations in the Swiss Alps by also accounting for occurrence of freeze–thaw events. We then employed a mixed-effects model to evaluate the respective contributions of morphological and climatic factors associated with frost drought.

2. Materials & methods

2.1. Study sites and available data

To assess the relevance of frost drought in mature trees growing in a natural environment, we selected a research setting with a multi-year stem size monitoring that provided continuous measurements of stem diameter variations and climatic conditions over a large ecological gradient and that included tree species with contrasting leaf behavior (evergreen and deciduous). The selected setting, located in the Lötschental valley (in the Swiss Alps, latitude = 46.39 and Longitude = 7.75), provided 14 years (2006 to 2019) of dendrometer and site environmental data from 40 mature *Picea abies* and *Larix decidua* trees from nine sites distributed along a 1400 m elevation transect (from 800 m asl up to the forest limit at 2200 m asl) from both north and south facing slopes (Fig. 1a). See King et al. (2013a,b) for a more detailed description of the research setting and Moser et al. (2010) for an in-depth analysis of the valley's climate.

Point dendrometers (type DR1, Ecomatik, Germany) were installed approximately 1.3 m above ground level on the north-facing section of the stem where the dead bark was removed. These dendrometers recorded stem diameter variation (SDV) with micrometer precision at 15-minute intervals, which were subsequently integrated to hourly resolution, covering the period from 2006 to 2019. These measurements were paralleled by site microclimatic variables collected at similar time resolutions to link tree growth physiology with environmental conditions. The microclimatic variables included, among others, air temperature and relative humidity (Tair and RH, measured at 2 m height, using HOBO U23 Pro v2, Onset USA), soil temperature (Tsoil, at 5 cm depth, HOBO tidbit v2, Onset USA), and stem surface temperature (at 1.4 m height, HOBO tidbit v2, Onset USA). These measurements have been complemented with daily estimation of evaporative pressure. Evaporative pressure was estimated using the variable of transpiration (VT) (Du et al., 2011; Kakubari and Hoskawa, 1992), obtained as the product of the daily vapor pressure deficit (daily mean VPD) and the squared root of daily solar radiation (Rs, as assessed using the *Annandale* model and corrected for elevation (Annandale et al., 2002), see Appendix). For a detailed distribution of these climatic variables in winter, see Fig. A.11.

2.2. Linking winter stem contractions to frost drought

In this study, we considered three different sets of conditions susceptible to lead to frost drought, i.e. loss of water due to evapotranspiration that is not compensated by water uptake (Table 1). Two of them are related to soil water uptake impairment, caused either by frozen (type 1, Tsoil < 0 °C) or by cold soil (type 2, Tsoil < 3 °C and VT > 1) under high evaporative pressure (see Fig. A.11 for the distribution of VT in winter). The third mechanism refers to water uptake impairment due to frozen stem, the ice blockage frost drought (type 3, frozen stem and VT > 0.3). For each of these variables, we then determined the number of days (number of hours divided by 24) for which these conditions occurred during the winter stem contraction (WSC) (Fig. 1b).

WSC was used as a proxy for stem water losses, based on the concept of tree water deficit (TWD), used for the growing season (Zweifel et al., 2005). TWD is calculated as the amount of stem contraction after detrending for stem growth. As stem growth does not occur in winter, we postulated that SDV, outside of freeze–thaw cycles, are directly related to the water status of the tree (the possibility of cellular death occurring during this period is discussed later). Consequently, winter stem contractions (WSC) were simply quantified for each tree and year (n = 40 x 14 = 520) as the total difference in stem diameter between its maximum in the previous autumn to early winter and its minimum in late winter to spring of the following year (Fig. 1b). This quantification was performed after smoothing the dendrometer time-series using a 24 h moving average. WSC was then corrected for the hygroscopic effect of the bark using the method developed by Delapierre et al. (2023) (see Appendix, Table A.2, and Fig. A.5). To avoid bias due to the specific SDV behavior during freeze–thaw cycles, the maximum and the minimum of WSC were defined outside such events.

Freeze–thaw cycles were identified by accounting for the environmental conditions necessary for their occurrence. Since apoplastic water in stems freezes between −2 and −6 °C and thaws above 0 °C (Davis et al., 1999; Zweifel and Häsler, 2000), we defined the onset of a freezing event when air temperature dropped below −3 °C for one hour, while for thawing the temperature should recover above 1 °C for 24 h (Fig. 1c). These values are overestimating freeze–thaw cycles on purpose to ensure that none of them will affect the interpretation of WSC. See Figs. A.12 and A.13 for the distribution of air temperature and estimated freeze-thaw cycles at the Lötschental transect.

In order to investigate the nature of diameter variations subsequent to a freeze–thaw cycle, we quantified freeze–thaw-related diameter change (ΔF) as the difference in diameter between the start and the end of a full freeze–thaw cycle. For that purpose, freeze–thaw cycles were defined by using the environmental conditions described above using a slightly stricter criteria (−3 °C for 8 h and 0.5 °C for 24 h for freezing and thawing, respectively). To precisely locate the onset and end of the freeze–thaw event, we targeted the abrupt contraction/swelling of the stem in response to freezing/thawing (Zweifel and Häsler, 2000). To do that, we calculated SDV differences from each time point to its neighbour and then applied a moving average with a window of 12 h to the SDV differences (aligned left/right for freezing/thawing, Fig. 1c). On this time series, peaks are related to periods of stem expansion and valleys are periods of stem contraction. Therefore, freezing events were expected to be located in the lowest valleys of this time series, whereas thawing events were located in the highest peaks. They were determined based on the 10% quantile of the lowest SDV differences for valleys and the 90% quantile of the largest SDV differences for peaks.

Table 1
The different frost drought conditions and their definition, see Fig. A.11 for the distribution of the soil temperature and VT.

Frost drought	Definition (subvariables)
Type 1 (frozen)	Unfrozen stem with soil temperature <0 °C
Type 2 (cold)	Unfrozen stem with soil temperature <3 °C & VT >1
Type 3 (ice blockage)	Frozen stem with VT >0.3

The freezing and thawing events were finally defined as the valleys and peaks that were the closest to the boundaries of the freeze–thaw events estimated based on temperature (see above). The precise start/end of the freezing/thawing event were defined as inflection points: Freezing events started at the first point with a positive value in the moving average time series prior to the selected valley, and thawing event at the first point with a negative value after the selected peak (Fig. 1c).

2.3. Data analysis

We used mixed models to investigate the drivers of both WSC and ΔF. The models were constructed in dependence of the frost drought variables (Table 1) and other relevant variables, such as species (*P.abies* or *L.decidua*), tree height and Diameter at Breast Height (DBH), using the R package *lme4* (Bates et al., 2015), with both the tree identifier and the site set as random effects (the first being nested within the latter). The output of the regression model was extracted using the R package *stargazer* (Hlavac, 2018). Both the normality and the homoscedasticity of the residuals were verified for the WSC mixed models. However, the distribution of the residuals for the ΔF mixed models showed a slight deviation from normality at the extremities. Mixed models R^2 were calculated using the R package *rsq* (Zhang, 2020).

3. Results

3.1. Drivers of WSC

The total winter stem contraction (WSC) ranged from 30 to 1478 μm. Contractions were larger in bigger trees (Pearson's correlation coefficient: R = 0.29 with DBH and R= 0.44 with Height) and at higher elevations, independently from slope exposure (Fig. A.6). WSC did not show any relation with the number of days of frost drought type 1 (Fig. A.7a), but exhibited a positive relation with both days under frost drought type 2 and type 3 (Figs. A.7b and A.7c). Results obtained from the mixed effects model (R^2 = 0.62) showed significant effects (P <0.0001) of species (*P.abies*), tree height and frost drought type 3 (Fig. 2a). Despite showing a positive correlation, the number of days (number of hours/24) under frost drought of type 2 emerged as a negligible model predictor.

3.2. Drivers of ΔF

About 75% of the freeze–thaw cycles resulted in stem contractions, measured as diameter change ΔF. Single event-related ΔF tended to slightly increase with elevation (Fig. A.8a). However, the seasonal sum of all ΔF (Seasonal ΣΔF) showed a more robust relation with elevation, suggesting a strong relation to WSC (Fig. A.8b). As such, WSC and ΣΔF were also strongly correlated (Fig. A.8c).

The analyses of the correlations of ΔF with transpiration-related variables indicated positive significant associations with the number of days where the transpiration variable VT > 0.3 (P<0.001), the maximum VT values, and tree height; as well as negative significant correlations (P<0.01) with the minimum temperature recorded during the freeze–thaw events (Fig. A.9). These results are also confirmed when these factors are pulled in a single mixed effects model (R^2 = 0.46) (Fig. 3b). However evaporative pressures (max VT, n daysVT > 0.3) have a stronger effect on ΔF than the minimum air temperature, which adds a maximum of about 100 μm (−4.55 × −25° C) to the modeled ΔF. The modeled species effect showed an increase for *P.abies* over *L.decidua*, similarly to the WSC mixed model, albeit not statistically significant.

4. Discussion

4.1. Frost drought as the main driver for WSC at the Lötschental transect

Our findings unveil that winter stem contraction (WSC) is predominantly attributed to contractions associated with freeze–thaw cycles (ΔF), and that these contractions are notably influenced by factors such as species (more pronounced in *Picea abies* trees compared to *Larix decidua* trees), and tree height (see Table A.3 for the height and DBH of individual trees). The extent of the contractions was strongly associated with evaporative pressures as well as the duration spent under freezing conditions.

Under the hypothesis that WSC is indeed a proxy for water losses (discussed in the next section), the combined effects of frost, tree height and evaporative pressures strongly suggest that the stem contractions are mainly a consequence of ice blockage frost drought, a type of water imbalance occurring when parts of the stem remain frozen while others are transpiring. Frost drought is likely to occur when there is a blockage to water uptake due to frost. This blockage can occur in the roots, or in the soil, but also in the base of the trunk (sometimes referred as to xylem ice blockages) (Mayr et al., 2012). Upon thawing, some parts of the stem will remain frozen longer. Sometimes, ice bodies can remain in the basal parts of the trunk a long time after most of the higher parts of the tree have thawed. Mayr et al. (2006) reported more than 110 freeze–thaw cycles on distal sun-exposed twigs and only 46 at the trunk (at 2 m height) of a 10 m high and 30 cm large (DBH) *P.abies*. Under high solar radiations, stem temperatures can reach well over 20 °C higher than the surrounding air temperature (Mayr et al., 2006b). These extreme temperature gradients can promote water loss through the cuticle and/or the periderm (Mayr et al., 2003b; Holtmeier, 2009). If parts of the trunk remain frozen, water uptake is inhibited and the water balance becomes negative (Mayr and Charra-Vaskou, 2007). Upon full thawing, frozen water in the trunk becomes available and is redistributed to the distal parts of the trees to balance the water losses. This phenomenon is greatly influenced by tree size, as it is based on differential thawing. A larger and taller canopy implies an increased surface of unfrozen distal parts submitted to water losses and a longer delay between distal and basal parts thawing (Mayr and Charra-Vaskou, 2007). In our study, freeze–thaw events were determined at the point of contact of the dendrometer, at about 2 m height of the stem. Considering that most trees in this study are considerably larger than the one presented by Mayr et al. (2006), it is most likely that distal parts of the trees have been undergoing thawing events, and thus water losses through transpiration, while the stem at the dendrometer height remained frozen. When the stem at dendrometer height is finally thawed, water is relocated to the distal parts, resulting in stem contraction and therefore positive ΔF values. Thus, even though water losses only concern sun-exposed distal twigs, they are ultimately detected at the stem at dendrometer height.

Such water losses would therefore be proportional the number of days under which these conditions may occur, to tree size (height) and inversely proportional to resistance to water losses. These predictions are confirmed by our results. In our case, WSC was more important for evergreen trees (*P.abies*), for which cuticular transpiration might occur than deciduous (*L.decidua*), for which only peridermal transpiration is possible.

However, this hypothesis raises an important question. If positive ΔF values were only caused by water losses, they should be reversible in nature, i.e. the tree should be able to recover and replenish its water reserve between the freeze–thaw events when all the xylem water is

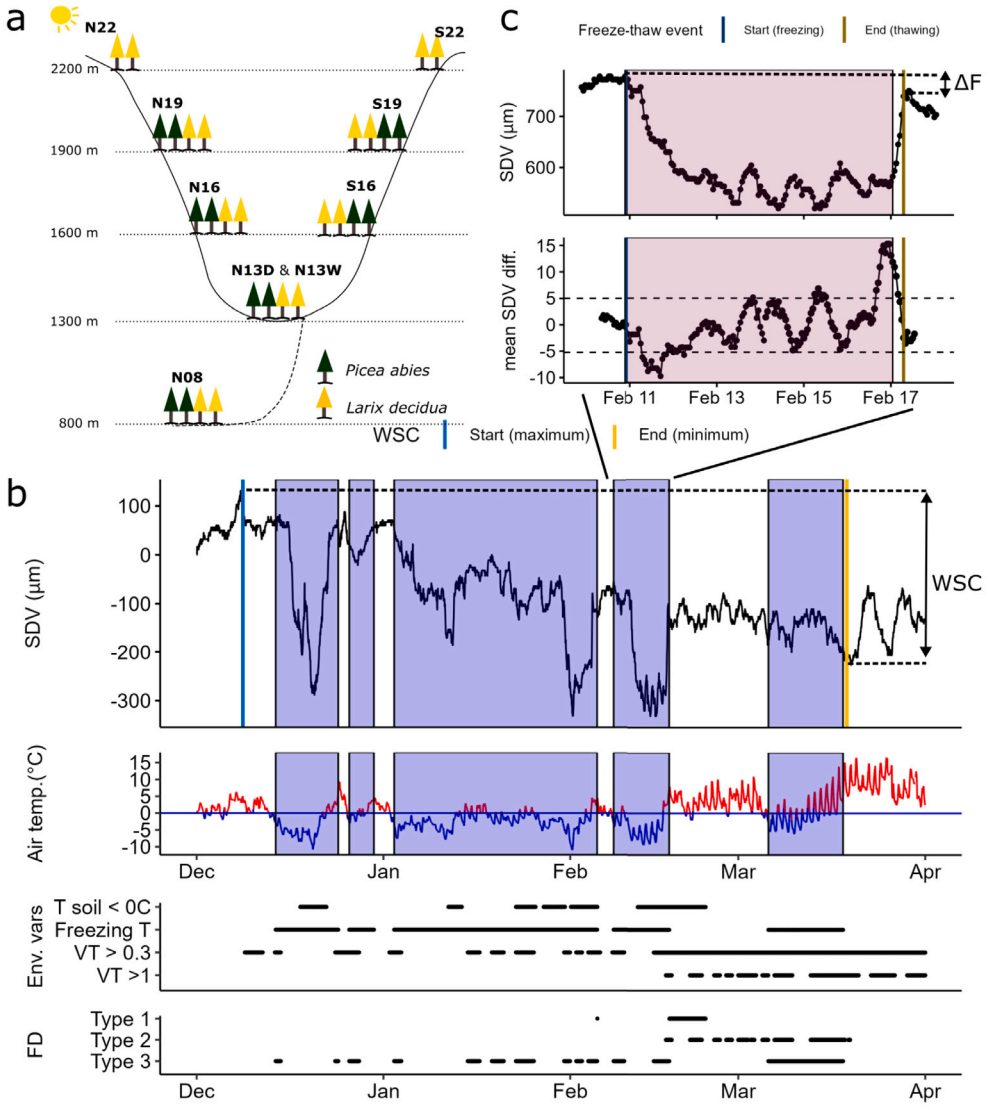

Fig. 1. Research setting and schematic for the calculation of Winter Stem Contraction (WSC) and freeze–thaw event related diameter change (ΔF). (a) Site settings at the Lötschental transect. (b) WSC calculation, environmental and frost drought variables (FD) for tree N08Ad_L1p (*L.decidua*) in the winter of 2009–2010. WSC is defined as the difference between the maximum diameter in autumn/winter and the minimum diameter in winter/spring the following year. Time periods where freeze–thaw events are susceptible to occur (blue boxes) are not considered. Negative air temperatures are shown in blue. (c) ΔF determination. ΔF is defined as the diameter differences between the start and the end of the freeze–thaw event. The purple box shows the estimated freeze–thaw event based on temperature. The dashed lines show peaks and valley thresholds. Blue and yellow lines shows inflection points and therefore the start and the end of the full event.

a

Predictor	Coefficient	Standard error
Height	19.25***	4.73
Species (*P.abies*)	117.29***	44.14
Frost drought type 2	-0.18	2.84
Frost drought type 3	8.86***	1.65
Constant	-255.01	156.73

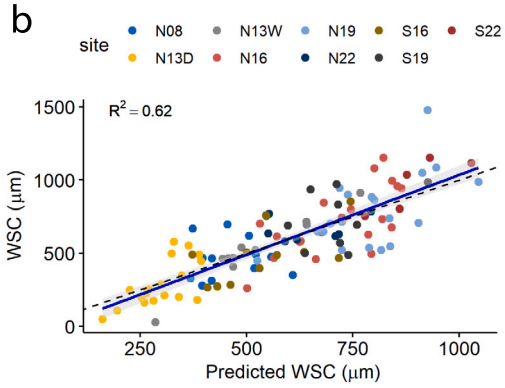

Fig. 2. Modeling WSC. (a) Model output table. Frost drought type are expressed in number of days (n hours/24), Species (*P.abies*) is the effect of this species over*L.decidua*. (***= P<0.001). (b) Predicted vs measured WSC. Dashed line shows 1:1 relation.

a

Predictor	Coefficient	Standard error
N days VT >0.3	8.71***	0.79
Max VT	46.51***	12.72
Min air temperature	-4.55**	1.53
Species (*P.abies*)	23.24	12.93
Height	3.69**	1.12
Constant	-185.57**	35.63

b

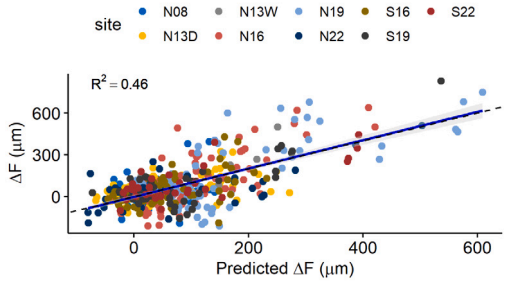

Fig. 3. ΔF mixed effects model with site and tree identification as random factors and height, species, and environmental variables showed in Fig. A.9 as fixed factors. (a) Model output table (**= P<0.01 ; ***= P<0.001). (b) Predicted vs measured ΔF. Dashed line shows 1:1 relation.

fully thawed. This would imply a swelling of the stem after each freeze–thaw event. Our results indicate that WSC is made up of the addition of ΔF and shows no signs of such rehydration (Fig. A.8c).

These results therefore point to limited or impaired water replenishment of the vessels during WSC. There are good indications that trees are unable to replenish their water reserve during this time period. Firstly, as negative air temperatures are prevalent in winter, the stem is frozen for months, often during most of the WSC time period, leaving only short-time windows for water uptake (Fig. A.10). Moreover, the time period during which the ice blockage occurs and thus water uptake is inhibited, most likely exceeds the "frozen" time detected in SDV, since the basal parts of the trunk (under dendrometer height at 2 m) can remain frozen even longer (Mayr and Charra-Vaskou, 2007). Secondly, even though soil temperatures rarely reach negative values, they remain low, most often well under 2 °C, during most of the WSC time period (Fig. A.10). At this temperature, water uptake is possible but can also be severely limited (Sakai and Larcher, 1987). For these reasons, it is therefore likely that the trees are only able to recover later in the season, when soil temperature or snow melting allows for water replenishment (Losso et al., 2021; Mayr et al., 2020) (Fig. A.10). Besides, the same pattern of winter contraction and spring re-hydration has been reported with non-frozen soils (Turcotte et al., 2009).

4.2. ΔF characterization and nature of the diameter change

Freeze–thaw events are very complex in nature. Ice nucleation and propagation can differ drastically in location and speed from one event to another (Charrier et al., 2017). Even though freeze–thaw events are visible in SDV, most prior studies that attempted to characterize them used either a controlled environment and/or in-situ phase shift detection methods (Améglio et al., 2001; Charra-Vaskou et al., 2016; Charrier et al., 2017; Lintunen et al., 2015). Here, we used a method of detection solely based on SDV. As a result, a certain margin of error is to be expected. In theory, freeze–thaw related SDV are either reversible, leading to null ΔF, or irreversible leading to positive ΔF. The negative ΔFs (about 1/4) are to be accounted for the imprecision of our method. However, we argue that the 3/4 of positive ΔF is also an indication that we successfully captured the most important events, such as the one shown in Fig. 1b.

In this study, we considered WSC, which consists mainly of the addition of ΔF, as water losses. However, prior studies have associated freeze–thaw irreversible diameter contractions with cellular death induced by ice nucleation within the cell (Améglio et al., 2001; Lintunen et al., 2015). Lintunen et al. (2015) used a climate chamber on several urban tree species to show that these irreversible changes are closely associated with the season and with the natural frost tolerance of the species. In their study, a winter freeze–thaw event with a minimal temperature of −17 °C did not trigger cellular death for every species. In light of these results, we suggest that cellular death, if present in our data (minimal temperature is a predictor ΔF), is not an important contributor to ΔF. Not only are the frost-hardy conifers of this study expected to be far more resistant to frost-induced cellular death, but most of the freeze–thaw events did not reach a temperature under −15 °C (Fig. A.9c). Moreover, if ΔF and WSC were mainly influenced by cellular death, we would not expect them to be related to evaporative pressures and the length of the freezing periods to such an extent.

If our results point towards the important contribution of water losses to WSC and ΔF, we cannot rule out that a certain portion of these variables are mechanical in nature and related to changes in the structure of the phloem tissues.

4.3. Ecological relevance of ice blockage frost drought

This study underlines for the first time the potential significance of the ice blockage frost drought. Some WSC reached over 1 mm, which is twice the water-related stem contraction commonly reported in summer (Oberhuber et al., 2015; Zweifel et al., 2005) and still greater than during singular summer drought events (Brinkmann et al., 2016). This result is in agreement with the numerous studies that have highlighted the significance of winter droughts at alpine treelines (Sakai and Larcher, 1987; Herrick and Friedland, 1991; Baig and Tranquillini, 1980; Mayr et al., 2006a; Sowell et al., 1996; Maruta et al., 2020).

Traditionally, winter droughts have been associated with the "classical" frost drought i.e. associated with cold and frozen soils (Sakai and Larcher, 1987; Tranquillini, 1982). We argue here that water losses are an inevitable consequence of freeze–thaw events, due to the physiology and the morphology of trees. Each freeze–thaw cycle creates at least a short time window of frost drought-like conditions due to differential thawing. The water losses during this phenomenon are less severe than during the "classical" frost drought because it occurs under limited evaporative pressure. Indeed, under stronger evaporative pressures due to high temperatures, the whole xylem water is likely to thaw, ending the constraint due to water uptake blockage. Because of these reasons, ice blockage frost drought should therefore be "chronic" in nature, in the sense that it occurs gradually over long periods of time (Larcher and Siegwolf, 1985).

Depending on the soil water status, freezing air temperatures can be either a protection or a facilitator of frost drought (Fig. 4). In unfrozen soils, like at the Lötschental transect, freezing air temperatures are provoking xylem water blockage, thus acting as a facilitator of frost drought. In frozen soils, where water uptake is already blocked, freezing air temperatures are limiting the extent of water losses through evaporation, thus acting as a protection against a more severe form of frost drought.

Another peculiar property of ice blockage frost drought is its timeline of occurrence. "Classical" frost drought has been linked with the end of winter and early spring, when the soil is still frozen and the

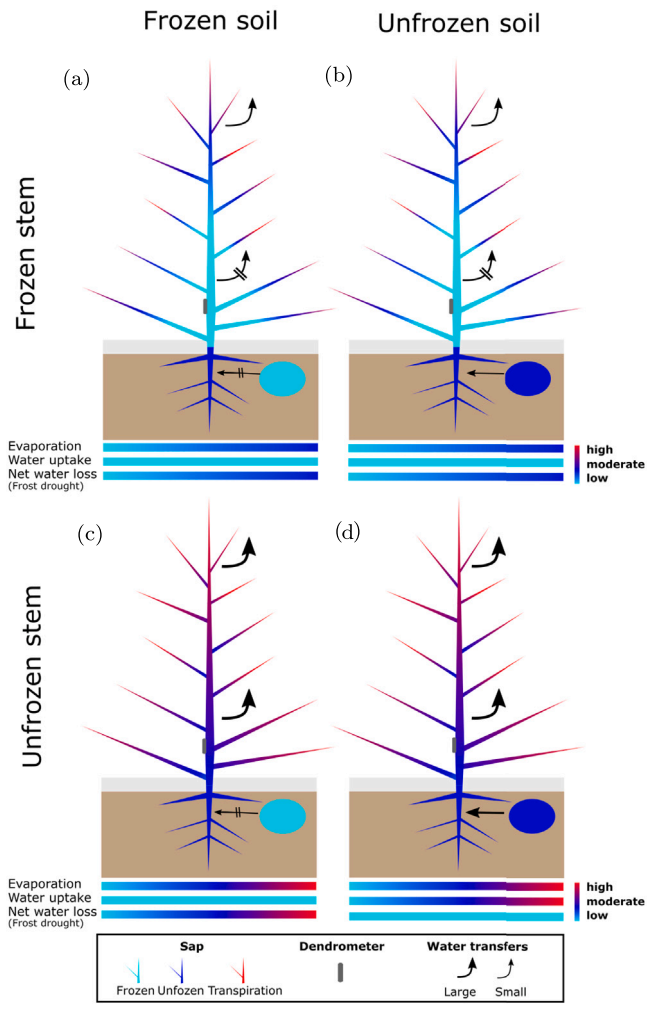

Fig. 4. Frost drought in relation to freezing conditions (design inspired by Charrier et al., 2017). Both A & B (frozen stem) are conditions where ice blockage frost drought is likely to occur. C shows conditions where "classical" frost drought is susceptible to occur. D shows conditions with no frost drought. Depending on the soil water status, freezing air temperatures are either a facilitator of or protection against frost drought : considering the net water loss, A < C but B > D.

evaporative demand is higher. However, ice blockage frost drought occurs already at the start of the cold season. We argue therefore that this phenomenon could be the reason treeline trees are already experiencing important water stresses and embolization in the middle of winter (Mayr et al., 2002; Maruta et al., 2020). Previously, freeze–thaw cycles related embolization has been linked with the formation and expansion of air bubbles in the xylem (Sperry and Sullivan, 1992; Mayr et al., 2003a). It is thus possible that water losses and therefore low xylem water potential are also an important contributor to freeze–thaw related embolization. This is supported by Ameglio et al. (2002) who reported that both freeze–thaw cycles and strong evaporative pressures during thawing are required for embolization to occur.

The geographical extent of this phenomenon remains to be assessed; it may be associated with or even specific to high elevations, where the combination of high solar radiation and high-temperature amplitudes favors both freeze–thaw cycles and cuticular/peridermal transpiration. It is possible that trees at the northern forest limits might not be experiencing such stresses due to the lack of thawing conditions. In boreal forests, where winter temperature often falls well under −40 °C, the primary concern is the damage induced by frost itself (Arris and Eagleson, 1989).

The important contribution of tree height to the phenomenon also raises the question of size limitation of conifers at alpine treelines. Previously, frost drought has been thought to affect young and small trees only, because bigger trees can rely on their water reserve to counterbalance the water losses (Körner, 2012). In the case of ice blockage frost drought, the question of size becomes paradoxical, as only bigger trees will be affected by significant water imbalances. Although we cannot tell whether these water losses are a threat to survival, they have likely driven alpine trees to evolve complex embolization repair mechanisms, such as the notable branch water uptake, replenishing the water-depleted distal parts in spring (Losso et al., 2021).

CRediT authorship contribution statement

Fabien Delapierre: Writing – review & editing, Writing – original draft, Methodology, Formal analysis, Conceptualization. **Christine Moos:** Writing – review & editing, Formal analysis. **Heike Lischke:** Writing – review & editing, Formal analysis. **Patrick Fonti:** Writing – review & editing, Formal analysis, Data curation.

Declaration of competing interest

The authors declare that they have no known competing financial interests or personal relationships that could have appeared to influence the work reported in this paper.

Data availability

Data will be made available on request.

Acknowledgments

We would like to thank Dr. Christophe Randin (University of Lausanne) for his input and expertise.

Appendix. Sample appendix section

A.1. Variable of transpiration

To assess the potential effect of frost drought on WSC, three frost drought variables were derived from air and soil temperatures, and the variable of transpiration (VT) (Table 1). VT relates to the evaporative pressure and includes both daily solar radiation (R_s) and the vapor pressure deficit (VPD). It has been used as a proxy for transpiration (Du et al., 2011; Kakubari and Hoskawa, 1992). It was calculated on a daily basis using the daily mean VPD (dVPD) and the equation :

$$VT = dVPD \times R_S^{1/2}$$

R_s s were modeled using the *Annandale* model which is derived from the *Hargreaves and Samani* model and corrected for elevation (Annandale et al., 2002) :

$$R_S = R_a \cdot A_{mod}(1 + 2.7 \times 10^{-5} \cdot Z)(T_{max} - T_{min})^{0.5}$$

A.2. Hygroscopic correction

WSC was corrected by subtracting the modeled hygroscopic response. The modeled hygroscopic response was calculated using the coefficients described in Table A.2 using the relation:

$$\text{Hygroscopic response} = \Delta\text{RH} \cdot \text{model RH slope},$$

with ΔRH being the difference in relative humidity between the start and the end of the WSC time period (Delapierre et al., 2023).

In most cases, the relative humidity was higher at the start than at the end of the WSC time period, resulting in positive values of ΔRH (Fig. A.5a). As expected, WSC is positively correlated with ΔRH, most likely as a result of the hygroscopic contraction of the stem (Fig. A.5b). The hygroscopic correction did not massively change the amplitude of WSC, with maximum corrections of about 200μm for the highest ΔRH values (Fig. A.5a). The corrected WSC relation with ΔRH becomes negligible when height is taken into account (Fig. A.5b).

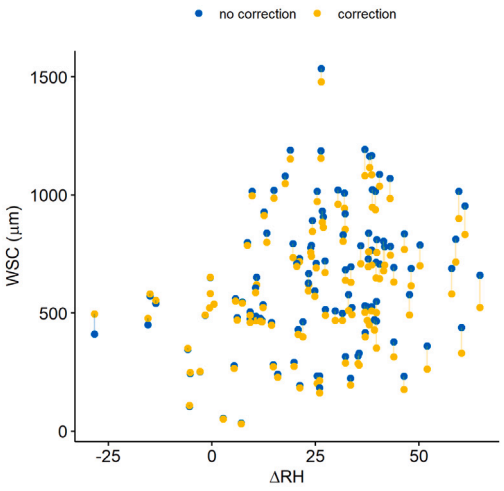

(a) Amplitude of the hygroscopic correction. Each point represents a tree.

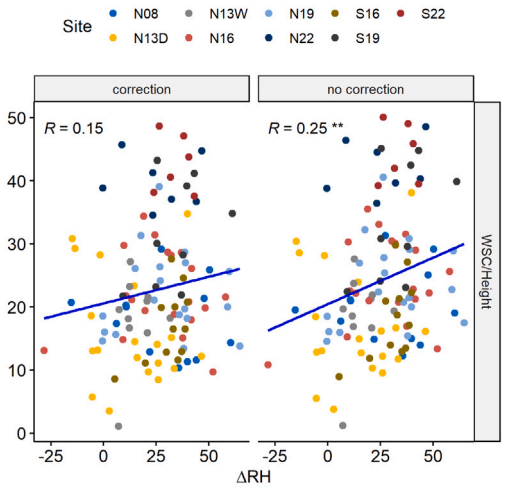

(b) Effect of relative humidity variation on WSC and hygroscopic correction in relation to height and DBH. R = Pearson's correlation coefficient, (*= P<0.05 ; **** = P <0.0001)

Fig. A.5. Hygroscopic correction for WSC in relation with height. The correction is based on the model developed by Delapierre et al. (2023). ΔRH is the difference in relative humidity at the start and the end of WSC.

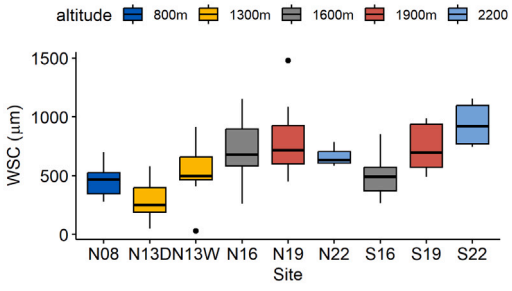

(a) WSC relation with site location.

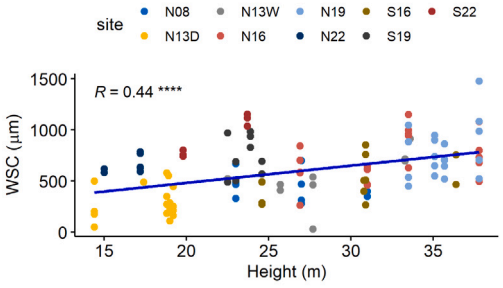

(b) WSC relation with tree height.

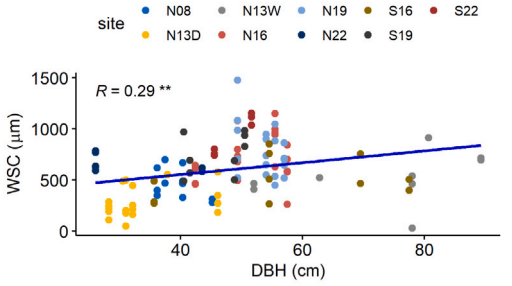

(c) WSC relation with Diameter at Breast Height (DBH).

Fig. A.6. Winter stem contraction (WSC) relation with location and morphological variables (**= P<0.01 ; ****= P<0.0001). Each dot represents the data of one tree and one year.

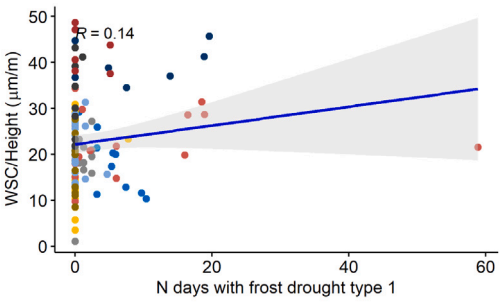

(a) Effect of frost drought type 1 on WSC

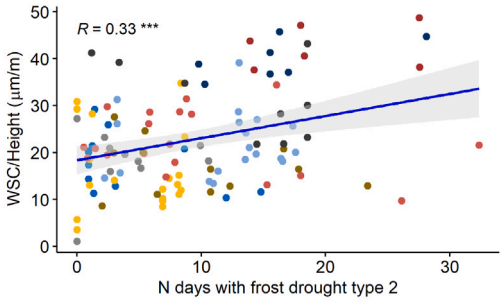

(b) Effect of frost drought type 2 on WSC

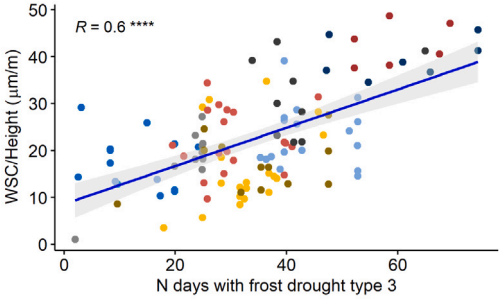

(c) Effect of frost drought type 3 on WSC

Fig. A.7. WSC in relation to frost drought types which are influenced by environmental variables. Each number of days when a given frost drought type occurs is counted over the WSC time period (between start and end). Each frost drought type is given by a unique combination of different micro-climatic subvariables representative of condition where frost drought is susceptible to occur (see Table 1). N days is the number of hours/24. R = Pearson's correlation coefficient, (**= P<0.01 ; *** = P <0.001 ; **** = P <0.0001).

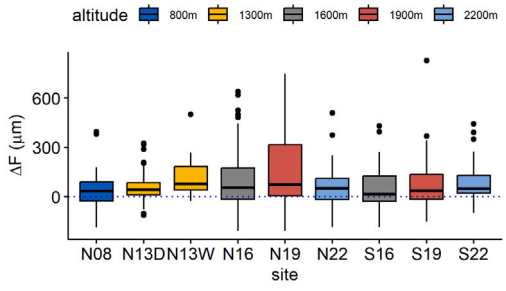

(a) Single (ΔF) and location

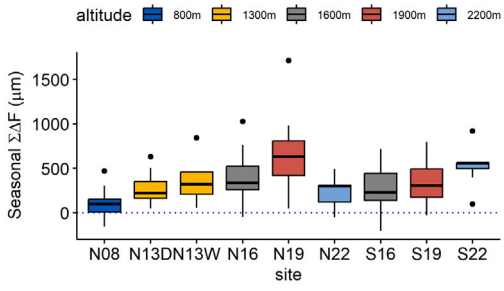

(b) Seasonal ΣΔFs and location

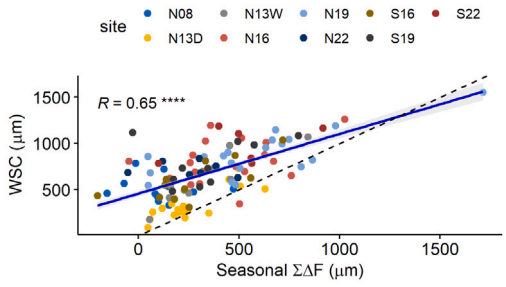

(c) Relation between seasonal ΣΔFs and WSC. Dashed line shows 1:1 relation. R = Pearson's correlation coefficient, (****=P<0.0001).

Fig. A.8. Freeze–thaw related diameter change (ΔF) in relation to location and WSC. Seasonal ΣΔFs is defined as the sum of all ΔFs for a whole winter.

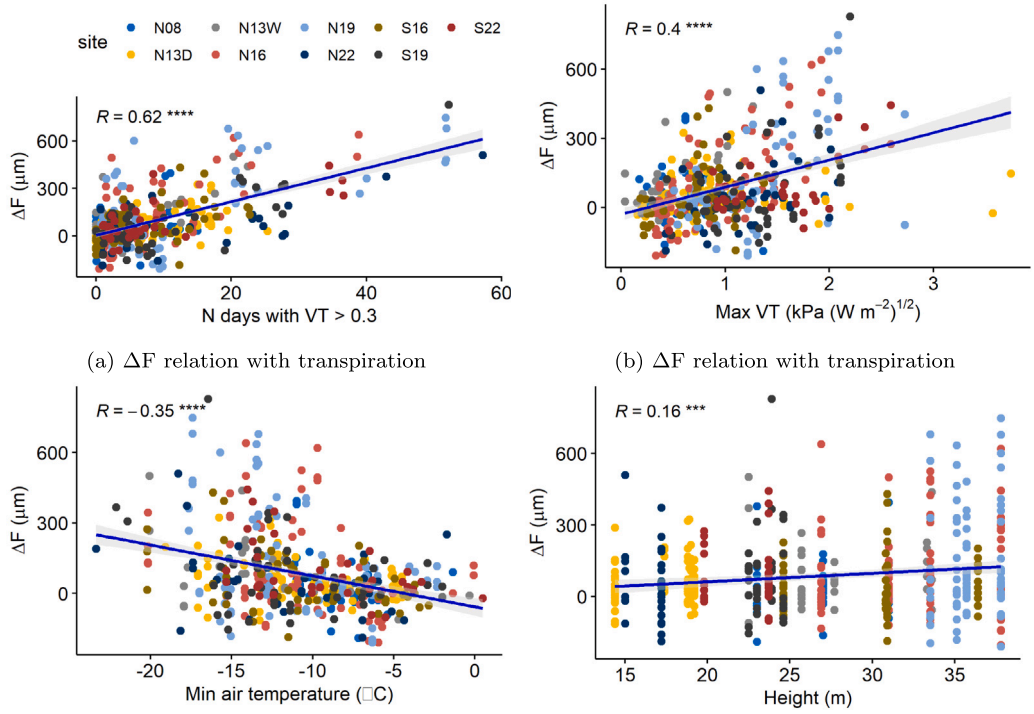

(a) ΔF relation with transpiration

(b) ΔF relation with transpiration

(c) ΔF relation with the minimum air temperature

(d) ΔF relation with tree height

Fig. A.9. ΔF in relation to environmental variables and tree height. Each environmental variable is derived over the full freeze–thaw event time period (between start and end). Each dot represents one tree in one freeze–thaw event. N days is the number of hours/24. R = Pearson's correlation coefficient, (****=P<0.001 ; ****=P<0.0001).

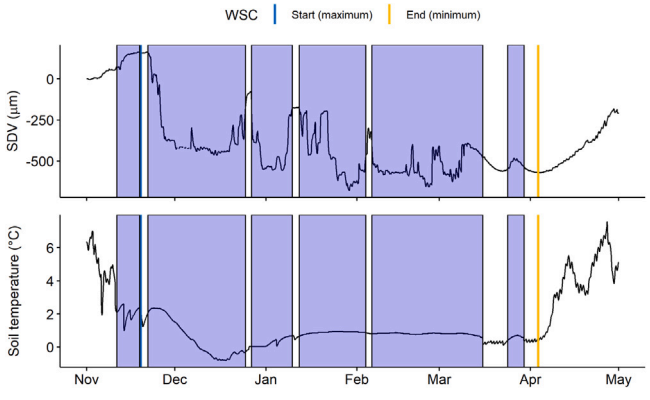

Fig. A.10. WSC time period with soil temperature of N13WD_L2p (*L.decidua*) during the winter of 2013–2014. Blues boxes indicate estimated freeze–thaw events. The SDV increase at the end of the season is concomitant with the rise of soil temperature.

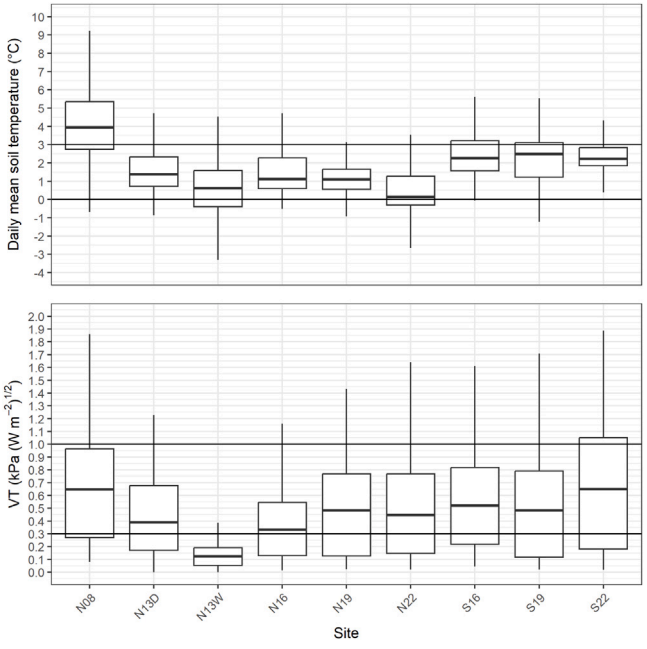

Fig. A.11. Distribution of daily mean soil temperature and VT at the Lötschental transect during winter (November, December and January) for the whole duration of the study (2006–2019). Horizontal bars show the values used to derive the frost drought variables (see Table 1).

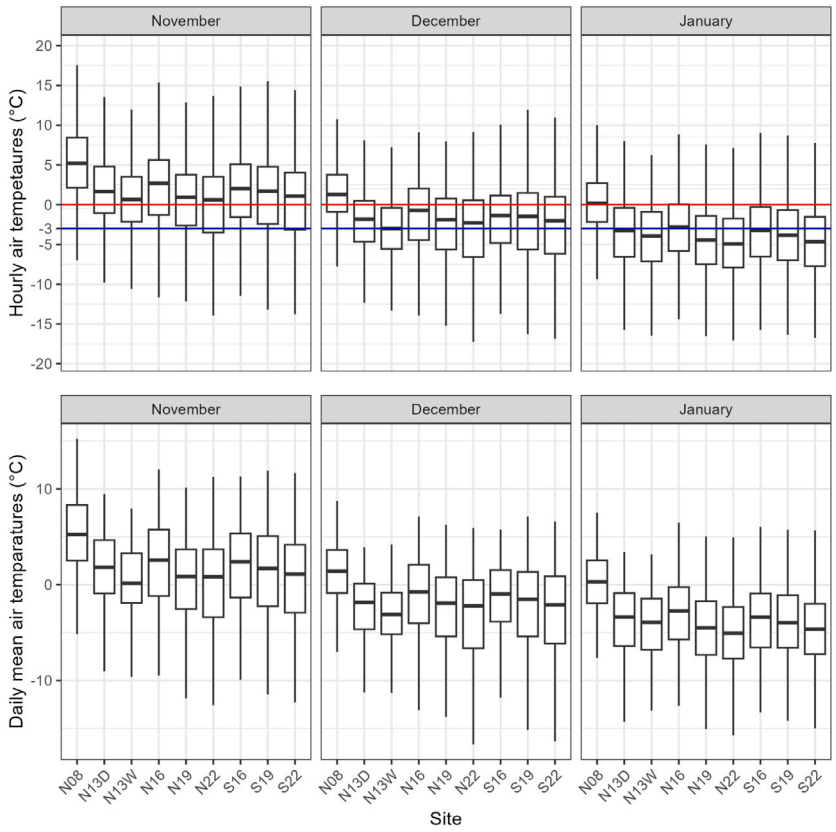

Fig. A.12. Distribution of air temperature at the Lötschental transect during winter for the whole duration of the study (2006–2019). Red and blue lines indicate temperature thresholds used to estimate freeze–thaw cycles statistics shown in Fig. A.13.

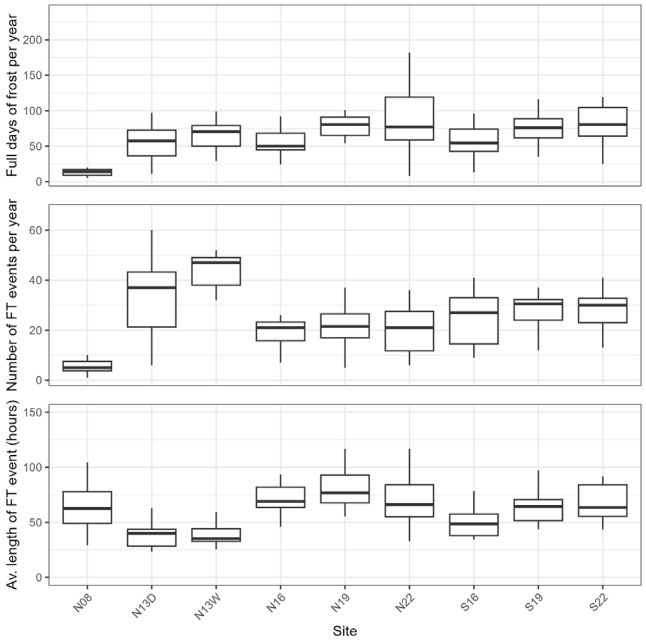

Fig. A.13. Statistics on estimated freeze–thaw cycles at the Lötschental transect for the whole duration of the study (2006–2019) (estimation solely based on temperature, thresholds are indicated by the blue and red lines in Fig. A.12).

Table A.2
Model parameters. Values derived using the following model : SDV = RH + mean temp. Delapierre et al. (2023).

Tree ID	Intercept	RH slope	Transp. slope
N08Ad_L1p	15.8	1.4	2.6
N08Ad_L4p	32.6	1.8	3.1
N08Bd_S3p	4	1.8	4.4
N08Bd_S4p	−3	32.9	4.8
N08Bd_S2p	−7.8	1.4	3.4
N13DAd_S1p	−2	1.2	1.4
N13DAd_S2p	2.8	0.5	1.8
N13DBd_L1p	−8	0.9	3.3
N13DBd_L2p	−11	0.8	4.1
N13DAd_L4p	−2.6	1.1	5
N13DBd_S3p	3.6	1	2
N13Wd_L1p	−2.3	0.5	1.2
N13Wd_S1p	−5.5	0.8	0.5
N13Wd_S2p	5.6	1	1.6
N13Wd_L2p	−11.3	0.6	4.6
N13Wd_L3p	−24.3	0.9	5.6
N13Wd_S3p	−7.6	1.1	0.3
N16Ad_L1p	36.1	1.5	2.5
N16Ad_L2p	19.8	1.9	3.1
N16Bd_S1p	24.6	3	2.6
N16Bd_S2p	43.2	2	0
N19Ad_L1p	25.3	1.9	4.5
N19Ad_L2p	20.4	1.6	3.6
N19Bd_S1p	42.2	2.1	1.9
N19Bd_S2p	47.2	1.8	4.5
N22Ad_L1p	13.2	2.1	3.9
N22Ad_L2p	24.4	1.4	4
S16Ad_L1p	49.7	1.4	2.9
S16Ad_S2p	−8.2	0.9	2.7
S16Bd_L1p	4.1	0.5	2.7
S16Bd_S2p	−18.4	2.1	5.2
S16Bd_L3p	−6.4	1.4	2.5
S16Ad_L4p	27.3	0	2.4
S19Ad_L1p	29.9	2	4
S19Ad_S2p	−7.5	1.7	19/6.3
S19Bd_L1p	−5.9	0.7	3
S19Bd_S2p	−2.7	0.9	4.7
S19Ad_L3p	−5.6	1.1	6.1
S19Bd_S3p	11	0.6	3.4
S22Ad_L1p	−7.5	0.9	4
S22Ad_L2p	−8.3	1.2	3.8

Table A.3
Tree size and diameter in 2015. The site is included in the first three characters of the tree's ID (see Fig. 1a).

Tree ID	DBH (cm)	Height (m)
N08Ad_L1p	45.2	27
N08Ad_L4p	37.4	27
N08Bd_S3p	40.3	23
N08Bd_S4p	36.1	31
N08Bd_L2p	41.5	26
N08Bd_S2p	36	25.8
N13DAd_S1p	31	14.4
N13DAd_S2p	46.1	18.8
N13DBd_L1p	28.2	19
N13DBd_L2p	32.1	19.2
N13DAd_L4p	30.5	17.4
N13DBd_S3p	37.8	18.9
N13DAd_L3p	38.7	19.2
N13DBd_S4p	40	18.2
N13Wd_L1p	78	27.7
N13Wd_S1p	81	29.5
N13Wd_S2p	62.8	22.5
N13Wd_L2p	89.3	33.3
N13Wd_L3p	52	25.7
N13Wd_S3p	80.7	33.6
N16Ad_L1p	42.4	31
N16Ad_L2p	57.5	26.9
N16Bd_S1p	49.3	37.8
N16Bd_S2p	55.5	33.5
N19Ad_L1p	54	35.1
N19Ad_L2p	57	35.7
N19Bd_S1p	49.3	37.8
N19Bd_S2p	55.5	33.5
N22Ad_L1p	43.5	15
N22Ad_L2p	26	17.2
S16Ad_L1p	36	25.7
S16Ad_S2p	35.6	24.6
S16Bd_L1p	77.5	30.8
S16Bd_L3p	69.5	36.4
S16Bd_S2p	54.5	30.9
S19Ad_L1p	50.5	23.9
S19Ad_S2p	40.5	22.5
S19Bd_L1p	48.8	23
S19Bd_S2p	41.5	24.6
S19Bd_S3p	36.5	24.9
S22Ad_L1p	45.5	19.8
S22Ad_L2p	51.6	23.7

References

Ameglio, T., Bodet, C., Lacointe, A., Cochard, H., 2002. Winter embolism, mechanisms of xylem hydraulic conductivity recovery and springtime growth patterns in walnut and peach trees. Tree Physiol. 22 (17), 1211–1220.

Améglio, T., Cochard, H., Ewers, F.W., 2001. Stem diameter variations and cold hardiness in walnut trees. J. Exper. Botany 52 (364), 2135–2142.

Annandale, J., Jovanovic, N., Benade, N., Allen, R., 2002. Software for missing data error analysis of Penman-Monteith reference evapotranspiration. Irrigat. Sci. 21 (2), 57–67.

Arris, L.L., Eagleson, P.S., 1989. Evidence of a physiological basis for the boreal-deciduous forest ecotone in North America. Vegetatio 82 (1), 55–58.

Baig, M.N., Tranquillini, W., 1980. The effects of wind and temperature on cuticular transpiration of Picea abies and Pinus cembra and their significance in dessication damage at the alpine treeline. Oecologia 47 (2), 252–256.

Bates, D., Maechler, M., Bolker, B.M., Walker, S., 2015. Fitting linear mixed-effects models using lme4. J. Statist. Softw. 67, 1–48.

Beikircher, B., Mayr, S., 2013. Winter peridermal conductance of apple trees: Lammas shoots and spring shoots compared. Trees 27 (3), 707–715.

Bozonnet, C., Saudreau, M., Badel, E., Améglio, T., Charrier, G., 2024. Freeze dehydration vs supercooling in tree stems: physical and physiological modelling. Tree Physiol. 44 (1), tpad117.

Brinkmann, N., Eugster, W., Zweifel, R., Buchmann, N., Kahmen, A., 2016. Temperate tree species show identical response in tree water deficit but different sensitivities in sap flow to summer soil drying. In: Phillips, N. (Ed.), Tree Physiol. 36 (12), 1508–1519.

Charra-Vaskou, K., Badel, E., Charrier, G., Ponomarenko, A., Bonhomme, M., Foucat, L., Mayr, S., Améglio, T., 2016. Cavitation and water fluxes driven by ice water potential in *Juglans Regia* during freeze–thaw cycles. J. Exper. Botany 67 (3), 739–750.

Charra-Vaskou, K., Charrier, G., Wortemann, R., Beikircher, B., Cochard, H., Ameglio, T., Mayr, S., 2012. Drought and frost resistance of trees: A comparison of four species at different sites and altitudes. Ann. Forest Sci. 69 (3), 325–333.

Charrier, G., Nolf, M., Leitinger, G., Charra-Vaskou, K., Losso, A., Tappeiner, U., Améglio, T., Mayr, S., 2017. Monitoring of freezing dynamics in trees: a simple phase shift causes complexity. Plant Physiol. 173 (4), 2196–2207.

Davis, S.D., Sperry, J.S., Hacke, U.G., 1999. The relationship between xylem conduit diameter and cavitation caused by freezing. Am. J. Botany 86 (10), 1367–1372.

Delapierre, F., Fonti, P., Lischke, H., Moos, C., 2023. A method to quantify and account for the hygroscopic effect in stem diameter variations. Front. Forests Global Change 6, 1167542.

Du, S., Wang, Y.-L., Kume, T., Zhang, J.-G., Otsuki, K., Yamanaka, N., Liu, G.-B., 2011. Sapflow characteristics and climatic responses in three forest species in the semiarid loess plateau region of China. Agricult. Forest. Meterol. 151 (1), 1–10.

Herrick, G.T., Friedland, A.J., 1991. Winter desiccation and injury of subalpine red spruce. Tree Physiol. 8 (1), 23–36.

Hlavac, M., 2018. Stargazer: Well-formatted regression and summary statistics tables. R Package Version 5 (2), 2.

Holtmeier, F.-K., 2009. Mountain timberlines. Springer.

Kakubari, Y., Hoskawa, K., 1992. Estimation of stand transpiration of a beech forest based on an eco-physiological computer simulation model and superporometer. J. Japanese Forestry Soc. 74 (4), 263–272.

King, G., Fonti, P., Nievergelt, D., Büntgen, U., Frank, D., 2013a. Climatic drivers of hourly to yearly tree radius variations along a 6°C natural warming gradient. Agricult. Forest. Meterol. 168, 36–46.

King, G.M., Gugerli, F., Fonti, P., Frank, D.C., 2013b. Tree growth response along an elevational gradient: Climate or genetics? Oecologia 1587–1600.
Körner, C., 2012. Alpine Treelines. Springer Basel, Basel.
Körner, C., 2019. No need for pipes when the well is dry—a comment on hydraulic failure in trees. Tree Physiol. 39 (5), 695–700.
Larcher, W., Siegwolf, R., 1985. Development of acute frost drought in Rhododendron ferrugineum at the alpine timberline. Oecologia 67 (2), 298–300.
Lindfors, L., Atherton, J., Riikonen, A., Hölttä, T., 2019. A mechanistic model of winter stem diameter dynamics reveals the time constant of diameter changes and the elastic modulus across tissues and species. Agricult. Forest. Meterol. 272–273, 20–29.
Lintunen, A., Paljakka, T., Riikonen, A., Lindén, L., Lindfors, L., Nikinmaa, E., Hölttä, T., 2015. Irreversible diameter change of wood segments correlates with other methods for estimating frost tolerance of living cells in freeze-thaw experiment: A case study with seven urban tree species in Helsinki. Ann. Forest Sci. 72 (8), 1089–1098.
Loris, K., Havranek, W., Wieser, G., 1999. The ecological significance of thickness changes in stem, branches and twigs of pinus cembra L. during winter. Phyton 39 (4), 117–122.
Losso, A., Bär, A., Unterholzner, L., Bahn, M., Mayr, S., 2021. Branch water uptake and redistribution in two conifers at the alpine treeline. Sci. Rep. 11 (1), 22560.
Maruta, E., Kubota, M., Ikeda, T., 2020. Effects of xylem embolism on the winter survival of Abies veitchii shoots in an Upper Subalpine Region of central Japan. Sci. Rep. 10 (1), 6594.
Mayr, S., Charra-Vaskou, K., 2007. Winter at the alpine timberline causes complex within-tree patterns of water potential and embolism in Picea abies. Physiol. Plantarum 131 (1), 131–139.
Mayr, S., Gruber, A., Bauer, H., 2003a. Repeated freeze–thaw cycles induce embolism in drought stressed conifers (Norway spruce, stone pine). Planta 217 (3), 436–441.
Mayr, S., Gruber, A., Schwienbacher, F., Dämon, B., 2003b. Winter-embolism in a“ krummholz” shrub (pinus mugo) growing at the alpine timberline. Austrian J. for. Sci. 120, 29–38.
Mayr, S., Hacke, U., Schmid, P., Schwienbacher, F., Gruber, A., 2006a. Frost drought in conifers at the alpine timberline: Xylem dysfunction and adaptations. Ecology 87 (12), 3175–3185.
Mayr, S., Schmid, P., Beikircher, B., 2012. Plant water relations in alpine winter. In: Lütz, C. (Ed.), Plants in Alpine Regions. Springer Vienna, Vienna, pp. 153–162.
Mayr, S., Schmid, P., Beikircher, B., Feng, F., Badel, E., 2020. Die hard: Timberline conifers survive annual winter embolism. New Phytol. 226 (1), 13–20.
Mayr, S., Wieser, G., Bauer, H., 2006b. Xylem temperatures during winter in conifers at the alpine timberline. Agricult. Forest. Meterol. 137 (1–2), 81–88.
Mayr, S., Wolfschwenger, M., Bauer, H., 2002. Winter-drought induced embolism in Norway spruce (*Picea Abies*) at the alpine timberline. Physiol. Plantarum 115 (1), 74–80.
Moser, L., Fonti, P., Büntgen, U., Esper, J., Luterbacher, J., Franzen, J., Frank, D., 2010. Timing and duration of European larch growing season along altitudinal gradients in the Swiss alps. Tree Physiol. 30 (2), 225–233.
Neger, F.W., 1915. Rauchwirkung, spätfrost und frosttrocknis und ihre diagnostik. Thar. Forstl. Jb 66, 195–212.
Oberhuber, W., Kofler, W., Schuster, R., Wieser, G., 2015. Environmental effects on stem water deficit in co-occurring conifers exposed to soil dryness. Int. J. Biometeorol. 59 (4), 417–426.
Sakai, A., Larcher, W., 1987. Frost survival of plants. In: Ecological Studies, vol. 62, Springer Berlin Heidelberg, Berlin, Heidelberg.
Schäfer, C., Rötzer, T., Thurm, E.A., Biber, P., Kallenbach, C., Pretzsch, H., 2019. Growth and tree water deficit of mixed Norway spruce and European beech at different heights in a tree and under heavy drought. Forests 10 (7), 577.
Sowell, J.B., McNulty, S.P., Schilling, B.K., 1996. The role of stem recharge in reducing the winter desiccation of Picea engelmannii (Pinaceae) needles at alpine timberline. Am. J. Bot. 83 (10), 1351–1355.
Sperry, J.S., Sullivan, J.E., 1992. Xylem embolism in response to freeze-thaw cycles and water stress in ring-porous, diffuse-porous, and conifer species. Plant Physiol. 100 (2), 605–613.
Tranquillini, W., 1979. Physiological ecology of the alpine timberline: Tree existence at high altitudes with special reference to the European alps. Ecological Studies, vol. 31, Springer Berlin Heidelberg, Berlin, Heidelberg,
Tranquillini, W., 1982. Frost-drought and its ecological significance. In: Physiological Plant Ecology II. Springer, pp. 379–400.
Turcotte, A., Morin, H., Krause, C., Deslauriers, A., Thibeault-Martel, M., 2009. The timing of spring rehydration and its relation with the onset of wood formation in black spruce. Agricult. Forest. Meterol. 149 (9), 1403–1409.
Wieser, G., Tausz, M. (Eds.), 2007. Trees at their upper limit: Treelife limitation at the Alpine timberline. In: Plant Ecophysiology, (v. 5), Springer, Dordrecht.
Zhang, D., 2020. Coefficients of Determination for Mixed-Effects Models. arXiv preprint arXiv:2007.08675.
Zweifel, R., Häsler, R., 2000. Frost-induced reversible shrinkage of bark of mature subalpine conifers. Agricult. Forest. Meterol. 102 (4), 213–222.
Zweifel, R., Item, H., Hasler, R., 2001. Link between diurnal stem radius changes and tree water relations. Tree Physiol. 21 (12–13), 869–877.
Zweifel, R., Zimmermann, L., Newbery, D.M., 2005. Modeling tree water deficit from microclimate: An approach to quantifying drought stress. Tree Physiol. 25 (2), 147–156.